Color-Line Vector Field for Multispectral Image Denoising

Mia RIZKINIA† Tatsuya BABA† Keiichiro SHIRAI‡ Masahiro OKUDA†
†The University of Kitakyushu
‡Shinshu University

Abstract The color-line feature defined as a line representing the shape of color distribution in a local region is often used in image processing. To demonstrate the practicability of the color-line concept for multispectral images, a new denoising method is proposed by the use of the color-line vector field and local color component decomposition, based on the extension of the RGB color line feature to M-band multispectral image. In contrast with most of conventional denoising methods which do not consider the correlation among the neighboring pixel colors, our method efficiently avoids discolorations by its color correlation consideration. The algorithm consists of color decomposition and filtering, iteratively. In the case of the multispectral images, the number of bands to process influences the calculation of the decomposed components. In this regard, our algorithm provides flexibility to set the number of processed band. The effectiveness of our method is validated by comparing the results to VBM3D and nonlocal means. Quantitative comparison shows that our proposed method produces superior results, and has closer similarity to the original image visually.

1 Introduction

Many denoising methods apply a procedure to RGB channels independently, which violates color balance and results in discoloration artifacts. To avoid this drawback, the color correlation should be considered and it can be approximated by the use of a color-line (cl) feature as an elongated cluster in the RGB color spaces that represents the shape of color distribution in a local region.

Some works introduce the application of cl feature. In [1], the cl features are used as a model to produce a new color representation. The work does not consider any particular color distortion, but precisely distinguishes one color from another by its cl feature. From this idea, they provide the use of cl model for some applications, i.e. segmentation, compression, color editing and saturated color correction in [1]. Whereas, Fattal et al. [2] exploit the cl pixel regularity of a single image to introduce a new dehazing method. They derive a local formation model reasoning the cl features in hazy scenes and describe how it is used for estimating the scene transmission.

Our previous work [3] introduced a novel smoothing and denoising algorithm based on the cl vector field produced from local color component decomposition step. The method successfully avoids discolorations that appear in the result of the compared method. Noise reduction based on cl is also introduced in [4]. They elaborate conventional filters such as the bilateral filter and nonlocal means, with the cl model to improve their performance. This research can significantly boost the conventional noise reduction capability.

Different from these applications that work on the RGB color image domain, in this paper, we extend the cl feature for RGB color image denoising to perform another color line application that is a new denoising method for multispectral satellite images. Denosing for multispectral image becomes a challenging problem due to the fact that it consists of more channel than RGB color image. By using the cl feature, our proposed denoising method considers the intensity correlation among neighboring pixels and among the bands. Hence, the denoising is conducted without ignoring the spectral information.

2 Algorithm

Our previous work [3] successfully introduced cl feature application for smoothing and denoising the RGB color image. In this paper, we improve the idea of cl feature to M bands image denoising and promote cl application for remote sensing area. In multispectral image case, we consider the intensity distribution of the M-band in local region. Basically, the proposed method works by iteratively filtering an image along the color line of its local color distribution.

The algorithm is illustrated in Figure 1. In detail, it consists of the following five steps:

1. Calculate the local color distribution of each pixel with their neighboring pixels as the color line vector fields (described in Subsec. 2.1).
2. Align the direction of each vector by changing the sign so that the neighboring vector directions become smooth (Subsec. 2.2).
3. Decompose each pixel into the mean color component, color line component, and residual component (Subsec. 2.3).
4. Do nothing to the mean color component and smoothing the color line component, and denoising the residual component (Subsec. 2.4).

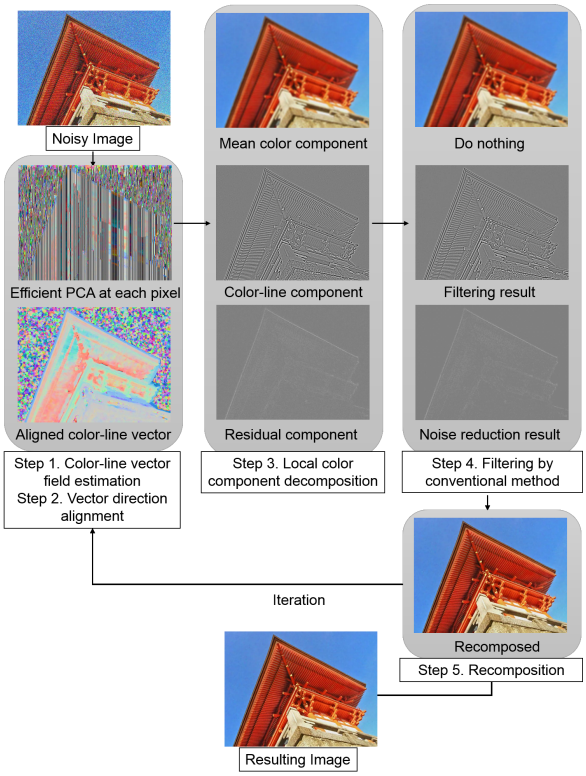

Figure 1: Flowchart of the proposed algorithm with four main steps conducted iteratively.

5. Reconstruct the image from its components. Turn back to step 1 (Subsec. 2.5).

2.1 Color Line Vector Field Calculation

We derive the *cl* vector as the eigenvector that corresponds to the maximum eigenvalue by using PCA. The more detailed procedure is given as follows:

1. Calculate the mean color component of each pixel i for each band,

$$\boldsymbol{\mu}_i = \frac{1}{w} \sum_{j \in \mathcal{N}(i)} \mathbf{I}_j \quad (i = 1, 2, \ldots, k), \tag{1}$$

where k is the number of pixels in the image, w is the number of pixels in a specified filter window $\mathcal{N}(i)$ and $\mathbf{I}_j = [I_j^1, I_j^2, \ldots, I_j^M]^\top$ is intensity of the neighboring pixels $j \in \mathcal{N}(i)$. Equation (1) produces the mean color that is $\boldsymbol{\mu}_i = [\mu_i^1, \mu_i^2, \ldots, \mu_i^M]^\top$.

2. Calculate the covariance of each pixel,

$$\mathbf{C}_i = \Big(\frac{1}{w} \sum_{j \in \mathcal{N}(i)} \mathbf{I}_j^\top \mathbf{I}_j \Big) - \boldsymbol{\mu}_i^\top \boldsymbol{\mu}_i, \tag{2}$$

that result in $\mathbf{C}_i \in \mathbb{R}^{M \times M}$.

3. To obtain the color line vector, find the maximum eigenvalue d_i of every pixel covariance $\mathbf{C}_i$, and subsequently derive its corresponding eigenvector as the *cl* vector $\mathbf{v}$.

2.2 Alignment of Color Vector Orientation

The resulting eigenvector $\mathbf{v}_i$ may have sign s_i in an ambiguity ($s_i = +1$ or -1), forming $s_i \mathbf{v}_i$. For the vector direction alignment, the sign s_i of a pixel i should be set to fit the dominant direction of neighboring vectors by using the inner product as the criterion. However, this step is only effective for pixel-wise flip. As for a large region of sign flip, a multiresolution approach is required.

Firstly, to determine the sign of each vector $\mathbf{v}_i$ that minimizes the energy function among neighboring pixel pairs $\{i, j\} : \sum_{\{i,j\}} \|s_i \mathbf{v}_i - s_j \mathbf{v}_j\|^2$, we adopt the following Jacobian relaxation method [5]:

$$s_p^{(t+1)} = sign\Big(\sum_{q \in \mathcal{N}(p),\ q \neq p} (s_p^{(t)} \mathbf{v}_p)^\top (s_q^{(t)} \mathbf{v}_q) \Big), \tag{3}$$

where the sign s_p of a pixel p is aligned with the dominant sign of 3×3 neighboring vectors in $q \in \mathcal{N}(p)$, considering the inner product.

Then, the step is followed by multigrid's V-cycle [5] as the multiresolution approach that is depicted in Figure 2. The multiresolution pyramid for vector and sign images is generated using Gaussian pyramid decomposition [6]. Additionally, in the decimation process, for the sake of giving the priority to pixels around edges which have large eigenvalues, we multiply the eigenvalue d_i as the weight for the pixel: $d_i s_i \mathbf{v}_i$, then apply the decimation filter and renormalize the half-sized vector field. As for the multiresolution eigenvalue images, they are generated by the same approach of the Gaussian pyramid.

2.3 Color Decomposition

The next step is the local color decomposition of each pixel color $\mathbf{I}_i$ into the *cl* component D_i (detail component) along the *cl* vector $\mathbf{v}_i$, and the

dual component N_i (noise component) perpendicular to it. This process is depicted in Figure 3. We begin with calculating the difference vector $\Delta \mathbf{I}_i = \mathbf{I}_i - \boldsymbol{\mu}_i$ to get the *cl* component as the inner product of the normalized *cl* vector,

$$D_i = \mathbf{v}_i^\top \Delta \mathbf{I}_i. \tag{4}$$

Then, we obtained the residual vector as,

$$\mathbf{r}_i = \Delta \mathbf{I}_i - D_i \mathbf{v}_i. \tag{5}$$

Finally, the residual component is derived from ℓ_2 norm of the residual vector,

$$N_i = \|\mathbf{r}_i\|. \tag{6}$$

2.4 Filtering

The *cl* components D_i obtained in the previous step still contain noise. Consequently, denoising of the *cl* components is required in the spatial domain. We iteratively refine the *cl* component which is in grayscale by denoising with the anisotropic diffusion [7]. We repeat

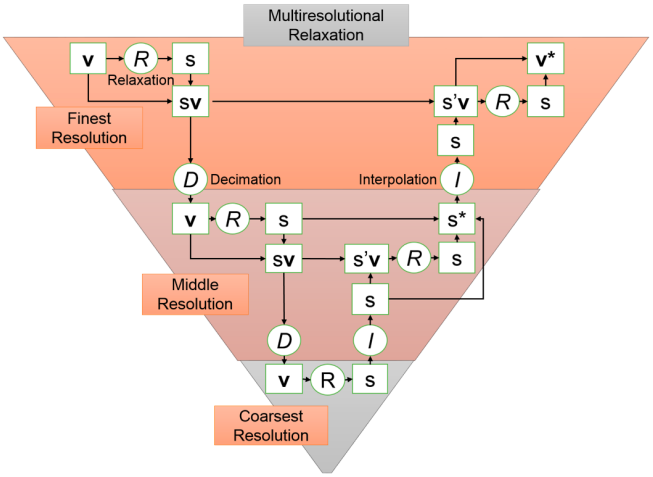

Figure 2: Multiresolutional relaxation method for vector direction algnment.

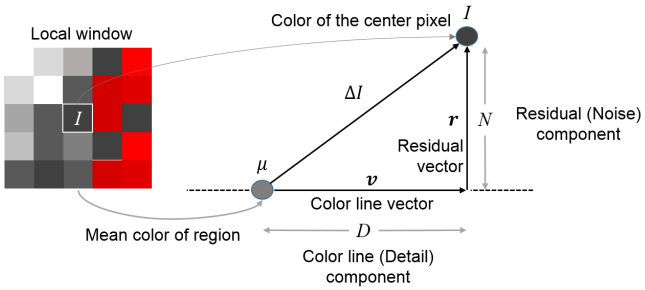

Figure 3: Color decomposition of one pixel.

the procedure until the desired criteria is met, resulting in the filtered *cl* component D_i. This conventional iterative filter is adopted instead of non-iterative filters such as conventional lowpass filters or median filters, since they perform too strong capability in smoothing. In other words, the anisotropic diffusion is more appropriate in our framework.

Meanwhile, the residual component N_i as the noise component is filtered using Geman McClure robust function [8] to reduce small intensity noise. Ultimately, the filtering step is followed by smoothing using Wiener filter giving the filtered residual component $\overline{N}_i$.

2.5 Reconstruction

The final step is color component recomposition to result in a smoothed and denoised image. The residual vector is normalized beforehand.

$$I_i = \boldsymbol{\mu}_i + \overline{D}_i \mathbf{v}_i + \overline{N}_i \mathbf{r}_i. \tag{7}$$

3 Experiment

The practicability of color line concept for multispectral image is examined by applying the proposed algorithm. To validate the effectiveness of our method, the results are compared to other powerful denoising methods, i.e. video block matching 3-D filtering (VBM3D) [9] and band-by-band nonlocal means (NLM) [10]. In the experiment, the parameters of our method and the competitor methods are set so as to give the best evaluation values.

Four real multispectral data are used in this experiment, i.e. the cropped area of Kyushu Island in Japan, Yellow River area in China, Papua Island in Indonesia and Washington in USA. They are collected by Operational Land Imager (OLI), and instrument onboard the Landsat 8 satellite. The multispectral band consists of band $1-7$, dedicated for coastal aerosol, red, green, blue, NIR, SWIR 1 and SWIR 2 channel respectively, with wavelength range $0.43-2.29\mu m$. Regarding this, the parameter M as the number of processed bands is set to 7. We contaminate the data by Gaussian noise with standard deviation of 0.06.resulting SNR of 24.44.

For the result evaluation, two quantitative parameter are taken, i.e. Peak Signal-to-Noise Ratio (PSNR) and Feature SIMilarity (FSIM). PSNR is popular as a ratio between the original image and the distorted image, where the higher the PSNR, the more similar the distorted image is to the original. As for FSIM, it exploits phase congruency and gradient magnitude as image low-level features that human visual system mainly recognizes from an image [11].

To calculate the color orientation, we use half of the window size which is set to 4. For the sake of the expected result, the number of main iterations is set to 3. The *cl* and residual component produced from the color decomposition step are shown in the top left and top right of Figure 4, respectively. Then, the *cl* component is processed to the smoothing phase using the anisotropic diffusion with 10 times iteration. Whereas, the residual component is denoised by our noise reduction filter. The image of each component after finishing the main iteration is illustrated in the bottom left and bottom right of Figure 4. The final images after the reconstruction are shown in Figure 5 and 6.

The experiment results are given in Table 1. Our method improves the image quality with PSNR reaching 10 dB increase than the noisy image. From the table, we can conclude that for all data, our method successfully achieves higher PSNR than the nonlocal means method and slightly competes the result of VBM3D. However, the significant superiority of ours compared with VBM3D can be distinguished from visual appearance depicted in Figure 5 and 6. These images illustrate, (a) original image, (b) noisy image with additional Gaussian noise, (c) result of nonlocal means method, (d) result of VBM3D, and (e) our iterative method with 3 iterations. One can see from these images that VBM3D results in too smooth images compared to the original, whereas our resulting images are closer to the original. Moreover, FSIM computation which correlates to the high informative features [11] yields higher value in ours than others.

(a) Cl component

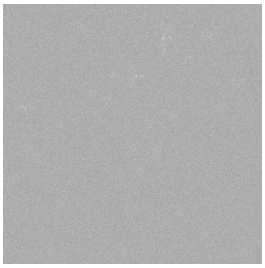

(b) Residual component

(c) Smoothed cl component

(d) Denoised residual component

Figure 4: Smoothing and denoising result of the decomposed components

4 Summary

In this paper, we have demonstrated that the color-line vector field along with the local color decomposition can be applied for multispectral image denoising corrupted by additive Gaussian noise. The basic idea of our method is exploiting the intensity correlation among bands and neighboring pixels to achieve the smoothed and denoised image. Our experiment show that the proposed method can compete with other powerful denoising methods, VBM3D and nonlocal means in both quantitative measurement and visual appearance comparison.

Acknowledgement

This work was supported in part by JSPS Grants-in-Aid (24560473), in part by the KDDI foundation, and in part by the Ministry of Finance, the Republic of Indonesia, under Indonesia Endowment Fund for Education.

Table 1: PNSR and MFSIM result (correspondents to first and second row of each data respectively).

Data	Noisy	NLM	VBM3D	Ours
Kyushu	24.4414	32.8880	34.2872	**34.3601**
	0.9423	0.9302	0.9457	**0.9706**
Papua	24.4414	31.7794	33.8546	**34.1661**
	0.9338	0.9408	0.9367	**0.9656**
China	24.4414	32.5792	34.3150	**34.4842**
	0.9469	0.9618	0.9740	**0.9809**
Washington	24.4414	29.5791	31.5495	**32.0093**
	0.9558	0.9721	0.9734	**0.9829**

References

[1] I. Omer and M. Werman. Color lines: Image specific color representation. In *Proc. IEEE CVPR*, pp. 946–953, 2004.

[2] R. Fattal. Dehazing using color-lines. *ACM TOG (Proc. SIGGRAPH)*, Vol. 34, No. 1, pp. 13:1–13:14, 2014.

[3] K. Shirai, M. Okuda, and M. Ikehara. Color-line vector field and local color component decomposition for smoothing and denoising of color images. In *IAPR Inter. Conf. ICPR*, pp. 3050–3053, 2012.

[4] W. Tu, C. Tsai, and S. Chien. Collaborative noise reduction using color-line model. In *Proc. IEEE ICASSP*, pp. 2465–2469, 2014.

[5] W. L. Briggs, V. E. Henson, and S. F. McCormick. *A Multigrid Tutorial: Second Edition*. Society for Industrial and Applied Mathematics, 2000.

[6] P. J. Burt and E. H. Adelson. The laplacian pyramid as a compact image code. *IEEE Trans. Commun.*, Vol. 31, pp. 532–540, 1983.

[7] D. Tschumperlé and R. Deriche. Vector-valued image regularization with pdes: A common framework for different applications. *IEEE Trans. Pattern Anal. Mach. Intell.*, Vol. 27, No. 4, pp. 506–517, 2005.

[8] M. J. Black and A. Rangarajan. On the unification of line processes, outlier rejection, and robust statistics with applications in early vision. *Int. J. Computer Vis.*, Vol. 19, No. 1, pp. 57–91, 1996.

[9] K. Dabov, A. Foi, V. Katkovnik, and K. Egiazarian. Image denoising by sparse 3d transform-domain collaborative filtering, 2007.

[10] A. Buades, B. Coll, and J. Morel. A review of image denoising algorithms, with a new one. *SIAM J.Multi. Model. Simul.*, Vol. 4, pp. 490–530, 2005.

[11] L. Zhang, L. Zhang, X. Mou, and D. Zhang. Fsim: A feature similarity index for image quality assessment. *IEEE Trans. Image Process.*, Vol. 20, No. 8, pp. 2378–2386, August 2011.

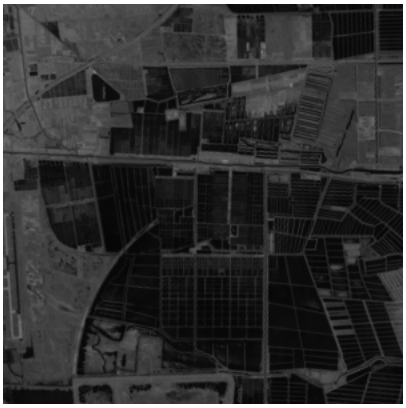

(a) Original (PSNR/MFSIM)

(b) Noisy (24.44/0.94)

(c) Nonlocal means (32.57/0.96)

(d) VBM3D (34.31/0.97)

(e) Ours (34.48/0.98)

Figure 5: Comparison among images from the experiment of China data band 5, with resolution of 30 m

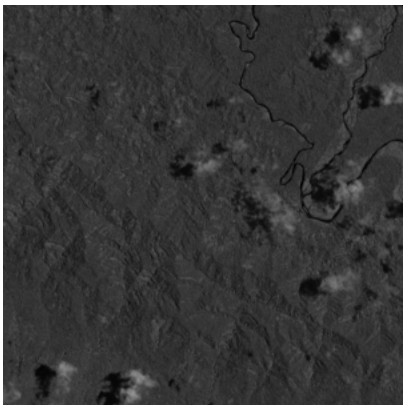

(a) Original (PSNR/MFSIM)

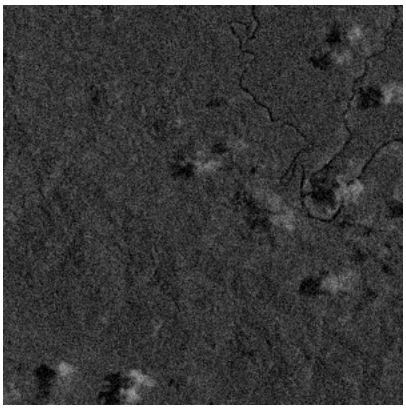

(b) Noisy (24.44/0.93)

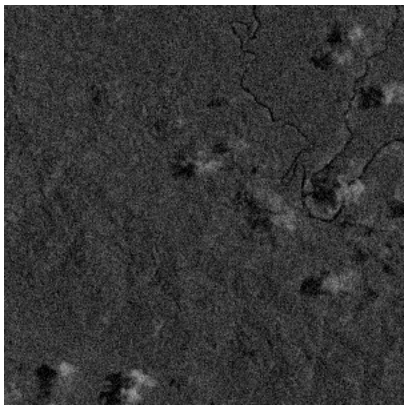

(c) Nonlocal means (31.77/0.94)

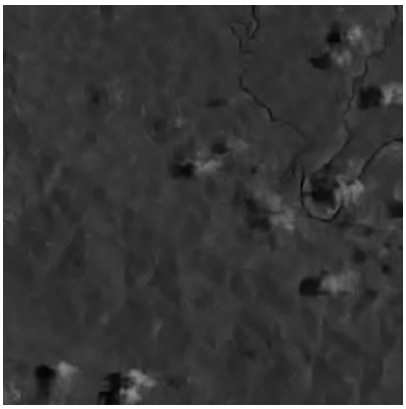

(d) VBM3D (33.85/0.93)

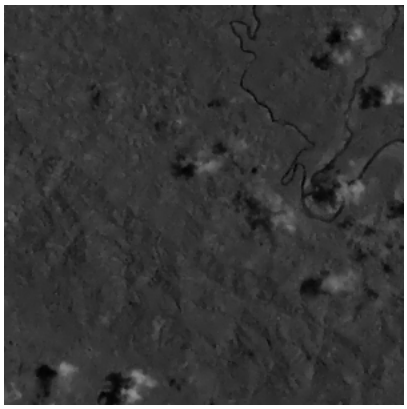

(e) Ours (34.16/0.96)

Figure 6: Comparison among images from the experiment of Papua data band 6, with resolution of 30 m.